Current Biology 21, 25–33, January 11, 2011 ©2011 Elsevier Ltd All rights reserved DOI 10.1016/j.cub.2010.12.016

Article

# Nuclear Geometry and Rapid Mitosis Ensure Asymmetric Episome Segregation in Yeast

Lutz R. Gehlen,[1,2,3] Shigeki Nagai,[1,2,4] Kenji Shimada,[1] Peter Meister,[1] Angela Taddei,[1,5] and Susan M. Gasser[1,*]
[1]Friedrich Miescher Institute for Biomedical Research, Maulbeerstrasse 66, CH-4058 Basel, Switzerland

## Summary

**Background:** Asymmetric cell division drives the generation of differentiated cells and maintenance of stem cells. In budding yeast, autonomously replicating sequence (ARS) plasmids lacking centromere elements are asymmetrically segregated into the mother cell, where they are thought to contribute to cellular senescence. This phenomenon has been proposed to result from the active retention of plasmids through an interaction with nuclear pores.
**Results:** To investigate the mother-daughter segregation bias of plasmids, we used live-cell imaging to follow the behavior of extrachromosomal DNA. We show that both an excised DNA ring and a centromere-deficient ARS plasmid move freely in the nucleoplasm yet show a strong segregation bias for the mother cell. Computational modeling shows that the geometrical shape of the dividing yeast nucleus and length of mitosis severely restrict the passive diffusion of episomes into daughter nuclei. Predictions based on simulated nuclear division were tested with mutants that extend the length of mitosis. Finally, explaining how various anchors can improve mitotic segregation, we show that plasmid partitioning is improved by tethering the plasmid to segregating structures, such as the nuclear envelope and telomeres.
**Conclusions:** The morphology and brevity of mitotic division in budding yeast impose physical constraints on the diffusion of material into the daughter, obviating the need for a retention mechanism to generate rejuvenated offspring.

## Introduction

Asymmetric cell division in single-celled organisms is thought to have arisen from the need for rejuvenation [1]. In multicellular organisms, asymmetric division drives the generation of different cell types and allows for the maintenance of pluripotent stem cells, thanks to an unequal distribution of cellular content during mitotic division [2]. Natural metabolic events generate damage to DNA, proteins, and subcellular organelles, the accumulation of which contributes to cellular aging [1]. The protection of germ cells and stem cells from an accumulation of damaged material is similarly thought to stem from differential segregation, which can be observed in both single- and multicelled organisms [3–5].

*Correspondence: susan.gasser@fmi.ch
[2]These authors contributed equally to this work
[3]Present address: Institute of Natural Sciences, Massey University, Private Bag 102 904, North Shore Mail Centre, Auckland, New Zealand
[4]Present address: Department of Structural Biology, Stanford University School of Medicine, 299 Campus Drive, Stanford, CA 94305-5126, USA
[5]Present address: Institut Curie, Centre de Recherche, and CNRS, UMR 218, F-75248 Paris, France

Aging in budding yeast is characterized by increases in generation time and size, a decline in mating ability [6, 7], and a switch to a state of hyperrecombination [8]. Most wild-type yeast strains enter terminal senescence after 20–30 divisions [9]. Importantly, the replicative life span of yeast daughter cells depends only weakly on the age of the mother [10], thereby allowing for an immortal cell population. Given that the mating of old cells and young cells yields diploids with a life span more similar to that of the older partner [6], it has been proposed that mother cells accumulate a "senescence factor" that cannot be transmitted to offspring [10].

Several factors, such as damaged proteins [8, 11, 12], dysfunctional mitochondria [13], and extrachromosomal DNA [3, 14], have been proposed to contribute to yeast senescence. In particular, extrachromosomal rDNA circles (ERCs) were found to accumulate spontaneously in aging mother cells [3]. Manipulations that either increase or decrease the amount of ERCs shorten or lengthen life span accordingly [15–18]. Similarly, aging can be accelerated by provoking the accumulation of a centromere-free autonomously replicating plasmid in the mother cell [14].

Although these studies provide considerable insight into the physiological consequences of asymmetric plasmid segregation in yeast, it remained unresolved why only one in ten plasmids passes into the daughter cell [19]. The volume ratio of mother to daughter nuclei is roughly 3 to 2 [20, 21] and therefore cannot alone account for this asymmetry. One explanation evokes an active mechanism of episome retention in the mother cell. Indeed, it was proposed that plasmids bind nuclear pore complexes (NPC), which were thought to be retained in the mother cell by a bud-neck impediment to nuclear membrane diffusion [22]. This model, however, was recently challenged by the demonstration that NPCs do efficiently migrate from the mother into the bud [23]. This argued that plasmid binding to NPCs is neither necessary nor relevant for the observed retention of ERCs in the mother cell [22, 23].

As an alternative and minimal hypothesis, we considered that the mother-daughter segregation bias of plasmids might arise passively from the geometry and kinetics of budding yeast cell division. It is clear that the daughter nucleus "grows" progressively out from the mother nucleus as a result of microtubule extension, and that the two nuclei stay connected by a thin tunnel until septation divides nuclei and cells. If a freely diffusing plasmid is allowed to equilibrate at mitosis, it will distribute with a frequency proportional to the nuclear volumes of mother and daughter. In contrast, if mitosis is too short for equilibration, the fact that the episome starts in the mother nucleus will lead to its retention in the mother cell. In that case, the geometry of the dividing nucleus itself might contribute to an apparent "diffusion barrier" that impairs episomal segregation. Consistent with this model is the fact that small 1.45 kb circles show less segregation bias than larger episomes [24]. To date, however, no one has directly tested whether asymmetric segregation occurs passively or as a result of active retention.

In this study, we investigated the plasmid segregation bias using live-cell imaging, mutants, and quantitative simulation studies of the segregation event. We show that an

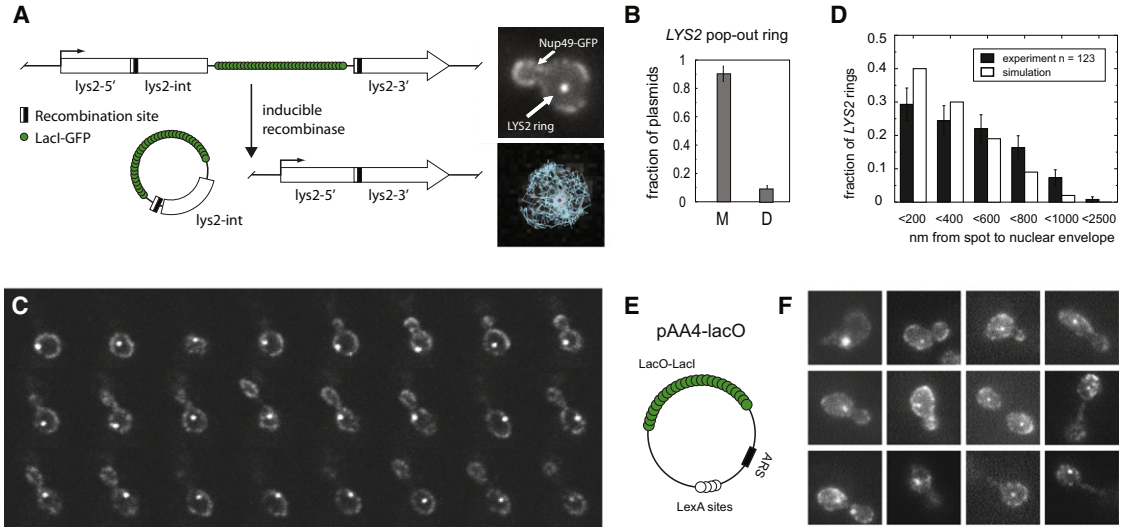


Figure 1. An Excised *LYS2* Ring and an ARS Plasmid Move Freely in the Nucleus yet Show a Strong Segregation Bias at Mitosis

(A) Yeast strain GA-2764 bears lacO and lexA binding sites at the chromosomal *LYS2* locus, integrated GFP-*lacI* and GFP-*NUP49* fusions, and a galactose-inducible R recombinase [25]. Growth on galactose induces excision of a 16.5 kb ring bearing 2.5 kb of *LYS2*, with 94% excision efficiency by 6 hr. Binding of GFP-lacI allows visualization of the ring, whose movement after 7.5 min is tracked in blue [25]. Time-lapse imaging of the episome is shown in Figure S1.

(B) Segregation bias of the excised *LYS2* ring after mitotic division. After 6 hr on galactose, 310 rings in either telophase or G1 phase cells were scored for presence in mother (M) versus daughter (D) nuclei. Error bars indicate standard error of the mean.

(C) Representative time-lapse images of mitotic cells bearing the excised *LYS2* ring. Image stacks were collected at 30 s intervals, and a partial-stack projection is shown.

(D) Distance from the excised *LYS2* ring to the nuclear envelope (GFP-Nup49) was scored for 123 cells and is plotted as a fraction of total rings scored (black bars). The standard deviation among independent cultures is shown and compared with a simulated random distribution (white bars).

(E) The pAA4-lacO plasmid was constructed by integrating 256 lacO sites into the pAA4 plasmid [26], which bears *URA3*, the 2 μm *ARS*, and an array of four lexA binding sites.

(F) The pAA4-lacO plasmid was not localized at the nuclear periphery during mitosis. Representative single confocal plane images of GA-1320 cells in mitosis are shown.

extrachromosomal ring and a plasmid carrying an origin of replication or autonomous replicating sequence (ARS) both move freely inside the nucleus yet show a strong segregation bias toward the mother cell. Computational simulations revealed that the shape of the dividing nucleus imposes a substantial constraint on episomal segregation by passive diffusion. Consistent with this model, we show that extending the duration of mitosis increases the probability that an ARS plasmid will be transmitted to the daughter cell. Mitotic segregation is similarly improved by episome attachment to the nuclear envelope or to telomeres. Our data argue that the mother-daughter segregation bias of episomes can be largely attributed to the brevity of mitosis and the structural burden at the bud neck; these impair the equilibration of centromere-free plasmids between mother and daughter nuclei. In addition, we validate a long-standing hypothesis that extrachromosomal DNA can associate with larger structures to pass "piggyback" into daughter cells, to enhance mitotic segregation.

## Results

### An Extrachromosomal *LYS2* Ring Moves Freely in the Nucleus yet Exhibits a Strong Mother Cell Bias

In order to examine the mechanism of the mother-daughter segregation bias of plasmids, we first monitored the dynamics of a 16.5 kb extrachromosomal ring of chromatin in mitotic nuclei. The chromatin, excised from the *LYS2* locus, bears an array of lacO sites that bind a GFP-lacI fusion and allows its visualization in living cells (Figure 1A; [25]). This episome does not have a functional origin of replication, and as a consequence, most cells do not contain more than one ring. With confocal imaging, we scored the presence of the *LYS2* episome in either mother or daughter nuclei and tracked its position relative to the GFP-Nup49-tagged nuclear envelope. Time-lapse imaging of either G1 or S phase cells at 1.5 s intervals shows the ring to be highly dynamic (Figure 1A; [25]).

To score the mother-daughter segregation bias of the excised *LYS2* ring, we monitored its presence in mother and daughter cells immediately after mitosis. At this point, the mother nucleus has on average 50% more volume than the daughter nucleus [21]. However, consistent with the segregation of ARS plasmids, we found 90% of the excised rings in mother nuclei and only 10% in daughter nuclei (Figure 1B), confirming earlier data which showed that only one in ten centromere-deficient plasmids passes to a daughter cell [19].

The excised *LYS2* ring has been shown to diffuse freely in G1 and S phase nuclei [25]. We extended this to G2/M phase cells using three-dimensional (3D) confocal stacks taken at 30 s intervals on cells traversing mitosis (see Figure S1 available online). The excised *LYS2* ring is highly mobile at mitosis, and visual inspection of the movies shows that it shifts position from frame to frame (Figure 1C). A mean squared displacement analysis (MSD; [25]) confirmed that its dynamics bear the characteristics of a freely diffusing particle in a spherical volume, with a radius of constraint of ~0.8 μm (Figure 2B), a value that approaches the average radius of a haploid yeast nucleus (~0.9 μm; [21]).

A recent report showed that a plasmid with an excisable centromere was associated with nuclear pores [22]. To see

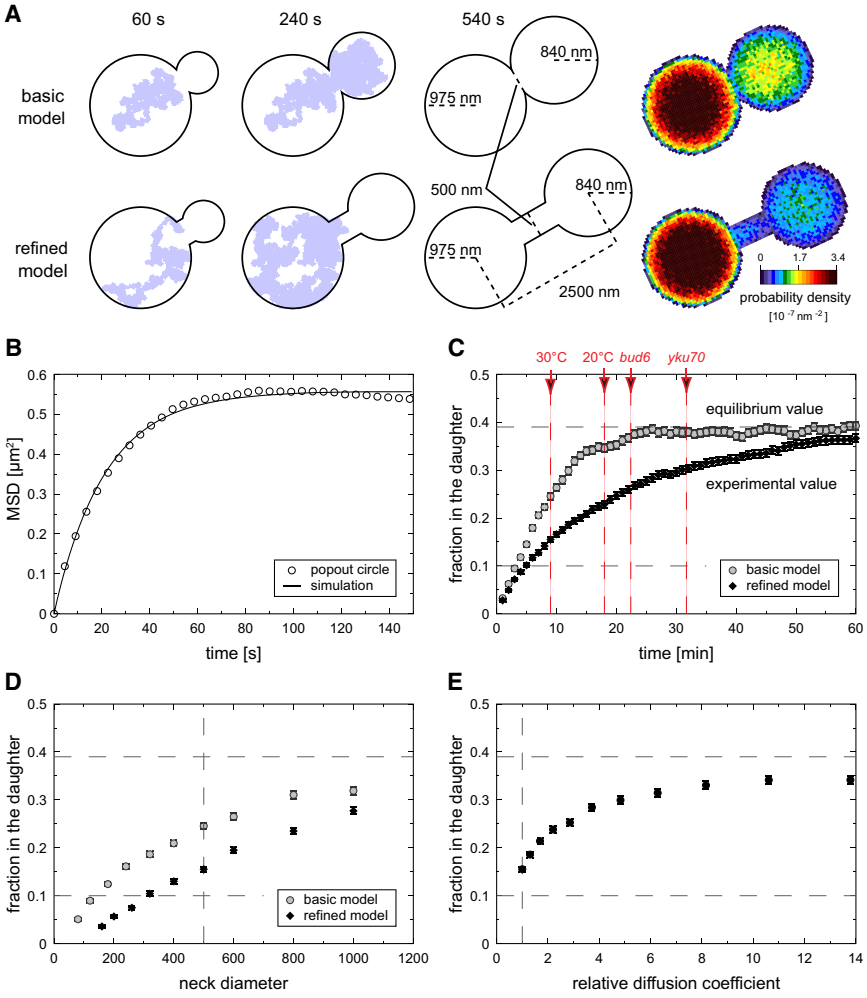


Figure 2. Physical Constraints of the Dividing Nucleus Inhibit Passive Diffusion to the Daughter Nucleus

(A) Planar view of the basic and refined model for the dividing nucleus at three different time points of nuclear division (see Figure S2 for images of yeast mitosis). The heat maps on the right show the projection of the probability density for the position of the plasmid at the end of mitosis, calculated from 200,000 independent simulations.

(B) Mean squared displacement analysis as previously published [25] compares excised *LYS2* rings with a simulated random walk in a spherical confinement. The agreement of the two curves allowed us to calibrate the time step of the simulation. A step size of 1 nm was used, with 44,602 steps per second.

(C) The fraction of plasmids in the daughter nucleus over time in the basic and the refined model, derived from 5,000 independent simulations each. Neither model equilibrates within 9 min; without the narrower tunnel structure between mother and daughter cells, one predicts 25% transmission to daughter nuclei by 9 min; with tunnel, 15%. The duration of mitosis in wild-type cells at 30°C and estimations for its duration at 20°C or in *yku70* or *bud6* mutants (at 30°C) are indicated with red arrows and dashed lines. The values for the two mutants were estimated based on the fluorescence-activated cell sorting (FACS) data shown in Figure 3A as $t(\text{mutant}) = n(G2/M_{\text{mutant}})/n(G1_{\text{mutant}}) \times n(G1_{WT})/n(G2/M_{WT}) \times 9$ min, where t is the duration of mitosis and n is the number of cells in the respective cell-cycle phase. The length of mitosis at 20°C was estimated based on the measurements by Vanoni et al. [32].

(D) The fraction of the plasmid in daughter nuclei is plotted against neck diameter in both models (n = 5,000 for each data point). A reduction of the diameter to 160 nm (40% of the default cross-section) in the refined model reproduces the experimental result.

(E) Fraction of transmission to the daughter is plotted against the diffusion coefficient (normalized to the default diffusion coefficient; n = 5,000 for each data point).

Error bars indicate standard error of the mean.

whether a neutral episome shows similar interaction, we measured the distance between the nuclear envelope (NE) and the *LYS2* ring in both G2 and mitotic cells and compared these measurements with the expected random distribution of a uniformly distributed particle simulated by computational modeling (Figure 1D; Figure S1). In contrast to the distribution reported in [22], the *LYS2* rings were slightly depleted from the nuclear periphery and showed no enrichment at the NE (Figure 1D). Moreover, their rapid and random movement was inconsistent with stable pore association (Figure S1). Nonetheless, they had the same mother cell segregation bias. We conclude that attachment to the NPC is not required for asymmetric distribution of episomes.

### An ARS Plasmid Also Moves Freely in the Nucleus

To test the possibility that ARS plasmids behave differently from the *LYS2* ring, a similar analysis was applied to a lacO-tagged ARS-containing plasmid, pAA4-lacO (Figure 1E). The pAA4-lacO plasmid contains 256 lacO sites, *URA3*, the 2 μm *ARS*, and four lexA binding sites and lacks a centromere, and the pAA4 plasmid has been shown to have strongly asymmetric mitotic segregation [26]. By coexpressing GFP-lacI and GFP-Nup49, we were able to readily visualize the position and number of plasmids per cell.

Visual inspection of cells transformed with pAA4-lacO showed that a small population contained many plasmids, whereas most cells were plasmid-free, consistent with the known segregation bias. We were able to find mitotic cells with only a few plasmids, which allowed us to monitor their individual movements in G2/M. In all cases, plasmids moved rapidly and were not found at the nuclear periphery (Figure 1F). The ARS plasmid dynamics were similar to those of the excised *LYS2* ring, suggesting that unconstrained diffusion may be a general feature of extrachromosomal circles that lack centromeres. This confirms a previous study showing that excised chromatin rings carrying an ARS have the same movement as those without one [25]. We conclude from these results that the high mobility of episomes does not overcome the strong mitotic segregation bias of budding yeast.

### Passive Diffusion and Geometric Constraint Are Sufficient to Induce a Segregation Bias

We next examined whether the geometric constraint imposed by the shape of the dividing nucleus effectively obstructs

episome transition to the daughter cell. We developed a computational model to investigate the effects of geometry, diffusion constant, and the duration of mitosis on the diffusion-based plasmid distribution. The plasmid is modeled as a particle diffusing freely inside the nucleus, which is initially spherical (i.e., as observed for both G1 and S phase). The daughter nucleus then bulges out of the mother with constant volume rate in late G2 and mitosis (Figure 2A, upper panel). We developed this model further with the following empirically determined parameters:

(1) Step size: Movement step size has to be small compared to the length scale of the confinement, which is on the order of hundreds of nanometers (see below). We found a detectable impact on the outcome of computer modeling if the step size value dropped from 10 to 5 nm, but there was no further change below 5 nm. We therefore used a value of 1 nm.

(2) Time step: We used tracking data from 3D rapid time-lapse imaging of the *LYS2* pop-out ring [25] to calibrate our simulation, by determining d, the distance moved over interval $\tau$, from experimental data. In order to do this, we fit the function $< d_1^2(\tau) > = a(1 - \exp(-\tau/b_1))$ to the MSD of the excised ring by varying a and $b_1$ (Figure 2B). We then simulated a random walk inside a spherical volume with the radius derived from the equation $R = (5/4a)^{1/2}$, which relates the value of the MSD plateau to the radius of constraint. We fit $< d_2^2(\tau) > = a(1 - \exp(-\tau/b_2))$ to the MSD of the walk by varying $b_2$, and the ratio $b_2/b_1$ gave the desired number of steps per second. For the step size of 1 nm, we used 44602 steps per second.

(3) Duration of mitosis: The duration of different sections of the budding yeast cell cycle has been measured by Lord and Wheals [27]. The time between the relocalization of the nucleus to the bud isthmus and the separation into two nuclei was measured as 8.8 ± 0.4 min (value used = 9 min) at 30°C.

(4) Radii of mother and daughter: The radii of mother and daughter nuclei directly after mitosis are $R_{mother}$ = 975 nm and $R_{daughter}$ = 840 nm, based on measurements of several hundred nuclei [21]. We used these values in our modeling and assumed that the daughter grows with constant volume rate.

(5) Final mother-daughter distance: As for the volumetric growth rate, we assumed that the center-to-center distance from mother to daughter nucleus would increase with constant speed. We measured the final center-to-center mother-daughter distance in 20 time-lapse movies and found that it varied from 2200 nm to 4200 nm. This stems from the inherent complexity of defining the end of mitosis precisely. This variability was later considered less of a problem, when tests showed that segregation efficiency depends much less on the final mother-to-daughter distance than on the neck diameter (data not shown). Therefore, the value used was 2500 nm.

(6) Neck diameter: The diameter of the neck between mother and daughter is crucial for our model, yet there has been no systematic study of this parameter using staining or imaging techniques to date. The use of fluorescent pore labeling to visualize the NE is not useful for determining neck diameter, because there are almost no pores in the neck. We therefore measured the diameter in published electron micrographs [20], which yielded a value of 450 nm. Modeling studies were then carried out with a range of neck diameter values around a default value of 500 nm (Figure 2D).

If freely moving plasmids were allowed to reach equilibrium under these empirically derived conditions, a plasmid would be recovered in 39% of the daughter cells, as a result of the mother-daughter volume difference. In our simulation, the episome reached only 25% of the daughter cells by 9 min. Simulations were run for longer times and were found to reach equilibrium by 25–30 min, a time that far exceeds normal yeast mitosis (Figure 2C). This result argues that mitotic plasmid segregation reflects a nonequilibrium state.

## A Refined Model Recapitulates the Observed Segregation Bias

The 25% transition probability determined by our modeling is nonetheless substantially higher than the 10% observed experimentally (Figure 1B). Our finding that the system is in a nonequilibrium state suggested that the precise geometry of the dividing nucleus might have a major impact on the extent of plasmid retention. We examined nuclear shape carefully and found that the nuclei appear to have a tunnel-like structure between two more spherical domains (Figure S2; [20]). Therefore, to more closely mimic the shape of the elongating mother nucleus, we introduced a tunnel between mother and daughter nuclei (Figure 2A, lower panel). Running the same simulation with this geometry of nuclear division led to a drop in transition probability to 15%, and a much longer time was needed to allow the system to equilibrate (Figure 2C).

The tunnel through which the plasmid diffuses to reach the daughter nucleus is not empty during mitosis but contains microtubules and chromosomes. Because these are likely to reduce the cross-section that is accessible to the plasmid, we ran a set of simulations in which we reduced the effective tunnel diameter (Figure 2D). Reduction of the diameter to 160 nm, or 40% of the original nuclear bud-neck cross-section, precisely recapitulated the experimentally observed value for plasmid segregation (10%). This demonstrates that the geometry of the dividing nucleus can determine the segregation rate of plasmids in a simulation based entirely on empirically determined values and passive episome diffusion.

Our model further predicts that the severity of the segregation bias will depend on the diffusion coefficient of the plasmid: a more rapidly diffusing plasmid should reach the daughter nucleus more efficiently [24]. We therefore tested the effect of an increased diffusion coefficient on the segregation bias. An episome's diffusion coefficient does not depend directly on its mass, but rather on its size and shape; thus, the diffusion coefficient of a 1.45 kb plasmid [24] could be up to 10 times higher than that of the 16.5 kb *LYS2* ring. Importantly, in a simulation that used a 10-fold higher diffusion coefficient, the segregation bias was nearly abolished (Figure 2E). Consistently, a strong reduction in the segregation bias was shown experimentally for a 1.45 kb replicating plasmid [24]. Thus, experimental data reinforce the robustness of our computer-based simulation.

## Extension of Mitotic Duration Improves Plasmid Partitioning

It follows from our model that the dividing yeast nucleus does not allow episomes to reach an equilibrium distribution before

nuclear separation. This observation predicts that conditions that prolong G2 or delay passage through mitosis should improve plasmid segregation into daughter cells (see Figure 2C). To test this hypothesis, we measured the stability of the ARS plasmid in a mutant with an extended mitotic duration via two well-established assays, mitotic stability and plasmid loss rate [26, 28]. Mitotic stability monitors the percentage of plasmid-bearing cells in a population under selective conditions [26], whereas plasmid loss rate is defined as the rate at which each dividing cell produces a plasmid-free daughter under nonselective conditions (see also [19]). Improved segregation efficiency for the plasmid results in increased mitotic stability and concomitant decrease in plasmid loss rate.

In order to test the effect of extending the G2/M transition, we used a *YKU70* deletion strain. Deletion of the smaller subunit of the yKu heterodimer (Yku70) leads to short telomeres and activation of the checkpoint kinase Chk1, which delays the G2/M transition (Figure 3A) [29, 30]. In wild-type cells, the pAA4 plasmid stability was 21%, with a loss rate of 0.3 (Figure 3B). *YKU70* deletion improved the mitotic stability of pAA4 to 31.5%, with a corresponding drop in plasmid loss rate to 0.15 (Figure 3B). Importantly, the double *yku70 chk1* mutant fully bypassed the G2/M delay (Figure 3A) and reversed the stabilizing effect (mitotic stability 18.8%, plasmid loss rate 0.27; Figure 3B), even though the double mutant still accumulated damage and released telomeres (data not shown). The mitotic stability and plasmid loss rate results are summarized in Table 1. They argue strongly that the diffusion of ARS plasmids into daughter cell nuclei can be improved by increasing the time available for plasmid transmission, and that the increased segregation could be separated from other effects of *yku70* deletion.

### Deletion of *BUD6* Improves the Segregation of the Freely Diffusing ARS Plasmid

A previous study argued that loss of the bud-neck protein Bud6 compromises a NE barrier that blocks the diffusion of nuclear pores into daughter nuclei, thereby allowing enhanced transmission of centromere-deleted episomes [22]. However, loss of Bud6 also extends G2/M (Figure 3A) [31]. We examined whether the effect of the *bud6* mutant is specific for a pore-associated plasmid by comparing the stability of the pAA4 plasmid in this mutant and its isogenic parent strain. As shown in Figure 1, the pAA4-lacO plasmid is highly mobile and is not associated with the nuclear periphery, yet the *bud6* deletion improved segregation of the pAA4 plasmid significantly: mitotic stability reached 40.6%, and plasmid loss rate dropped to 0.23 (Figure 3C; Table 1). This was not restricted to the ARS-containing plasmid. We also scored the efficiency of transfer of the freely diffusing *LYS2* rings in the daughter nucleus after mitosis in wild-type and *bud6* deletion strains. Like pAA4-lacO, the excised *LYS2* ring was transferred into the daughter nuclei more efficiently in the *bud6* mutant (Figure 3D).

Because freely diffusing plasmids have no pore association to lose, we suggest that the effect of the *bud6* mutation on plasmid stability indeed reflects its significantly extended G2/M phase (Figure 2C; Figure 3A). Indeed, two mutants (*yku70* and *bud6*) that extend G2/M through different mechanisms both increase plasmid segregation efficiency. This supports our hypothesis that the brevity of mitosis combined with the passive diffusion of episomes jointly leads to a mother cell bias in centromere-free episome segregation.

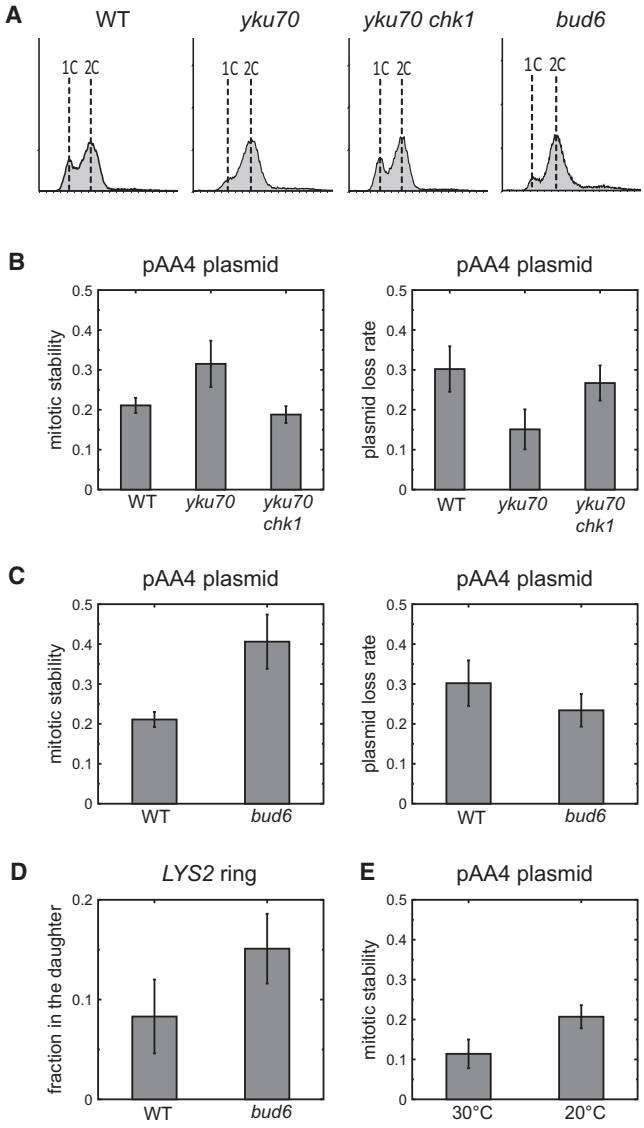


Figure 3. ARS Plasmid Segregation Is Improved by Extending the Duration of Mitosis

(A) FACS analysis showing DNA content for unsynchronized populations of wild-type (GA-180) and isogenic strains bearing deletions of *yku70* (GA-2661), *yku70 chk1* (GA-3992), and *bud6* (GA-3814). Mutants *yku70* and *bud6* accumulate in G2/M.

(B) Effect of *yku70* and *yku70 chk1* deletion on pAA4 plasmid stability. Mitotic stability and plasmid loss rates are shown. The average of six trials with independent transformants is given.

(C) Mitotic stability of the pAA4 plasmid was monitored in the *bud6* deletion under conditions as in (B).

(D) Fraction of excised *LYS2* rings in the daughter nucleus after mitosis in a wild-type (GA-2764; n = 60) and *bud6* deletion strain (GA-3816; n = 126).

(E) The effect of growth temperature, which doubles the time of G2/M, was scored for pAA4 plasmid stability. Mitotic stability of the pAA4 plasmid was monitored at the indicated temperatures, under conditions otherwise identical to those in (B). Rates shown are the average of six trials with independent transformants.

Error bars indicate standard error of the mean.

In a final test of our hypothesis that segregation is a diffusion-limited process, we monitored the mitotic stability of pAA4 at different temperatures. The yeast cell cycle is reproducibly extended by growth at lower temperature, and the

Table 1. Partitioning of the pAA4 Plasmid in Different Mutants

| Genotype | Mitotic Stability (%) | Plasmid Loss Rate |
|---|---|---|
| wild-type | 21.1 ± 1.9 | 0.30 ± 0.06 |
| *yku70* | 31.5 ± 5.8 | 0.15 ± 0.05 |
| *yku70 chk1* | 18.8 ± 2.1 | 0.27 ± 0.04 |
| *bud6* | 40.6 ± 6.8 | 0.23 ± 0.04 |

Data are presented as mean ± standard deviation.

length of G2/M doubles when growth temperature is shifted from 30°C to 20°C [32]. At the same time, diffusion rates can be expected to be slightly slower. Using the assumption of the Stokes-Einstein relation [33], we calculated that the diffusion coefficient D should be reduced to roughly 80%, assuming that the nucleoplasm shows the same temperature dependency as water [34]. By computer simulation, taking into account both the reduced diffusion coefficient (D) and the extended G2/M, we predicted that the fraction of daughter cells receiving plasmids should be 20.1% (Figure 2C). Although this is a modest increase, and although we cannot rule out indirect effects of temperature, this prediction was borne out by experimental assay. The mitotic stability of pAA4 in wild-type cells was scored as 20.7% at 20°C as compared to 12.3% at 30°C (Figure 3E). Taken together, our data suggest that extended duration of mitosis improves plasmid partitioning, consistent with our modeling of a diffusion-limited process. The experimental values determined for these various conditions agree well with the numbers predicted from the simulation of episome segregation and the extension of the cell cycle estimated for each condition (Figure 2C, red arrows).

## Anchoring to the Nuclear Envelope Improves Plasmid Partitioning

These simulations and mutant analyses argue that there is no requirement for active molecular retention to explain the strong segregation bias of episomes in budding yeast. Instead, we propose that the cell needs an active mechanism to overcome its inherent segregation bias. We tested this by examining the mechanisms that lead to the symmetric segregation of a centromere-free episome.

Previous studies had shown that the addition of subtelomeric or telomeric sequences [28], the binding of Rap1 and Sir4 [28, 35], and the targeting of a small partitioning and anchoring domain (Sir4PAD; [26, 36]) directly improve the mitotic segregation of an ARS plasmid. The PAD domain of Sir4 is known to anchor silent chromatin and telomeres to the NE [37]; thus, it could link the plasmid to either telomeres or the nuclear periphery. Arguing for NE association, the Sir4PAD-mediated enhancement of ARS plasmid segregation has been shown to require interaction with Esc1 [36]. Nonetheless, other explanations, such as local recruitment of nucleosome-modifying enzymes like Sir2 or an association with heterochromatin per se, have not been ruled out.

To test whether simple tethering of an episome to the NE enhances mitotic segregation, we targeted a fusion of lexA with the integral membrane protein Yif1 to the plasmid. LexA-Yif1 has been shown to relocate an internal GFP-tagged chromosomal locus to the NE in yeast interphase cells [37]. We confirmed that lexA-Yif1 also tethers a tagged internal sequence (*ARS607*) to the inner nuclear membrane in G2 phase cells (Figure 4B). Moreover, the lexA-binding *LYS2* ring showed enhanced NE association in mitosis only when lexA-Yif1 was bound (Figure S3). To test the effect of this neutral NE anchoring on plasmid partitioning, lexA-Yif1 was targeted to pAA4. Like lexA-Sir4PAD, lexA-Yif1 improved pAA4 mitotic stability and reduced plasmid loss rate (Figure 4C). The effect of lexA-Sir4PAD required the Sir4 ligand Esc1, whereas that of lexA-Yif1 did not (Figure 4C; [37]). Stabilization also required the direct binding of the lexA fusions to the episome, because a plasmid without lexA sites (pAA0) was unaffected (Figure 4D). These results are summarized in Table 2. We ruled out that the possibility that improvement in plasmid stability arose from enhanced replication efficiency by determining average plasmid copy number on Southern blots (Figure S4). We conclude that plasmid stability in yeast can be improved by anchoring the plasmid to the NE. This is consistent with the observation that inner nuclear membrane proteins [22] and nuclear pores [23] transit efficiently with the NE into the daughter nucleus during mitotic division. Indeed, recent work from Khmelinskii and colleagues ([38], this issue of *Current Biology*) shows that anchorage to nuclear pores itself improves segregation efficiency.

Why should association with the NE enhance segregation of an episome? The mathematical theory of narrow escape [39] predicts that the time that a diffusing particle needs to escape from a spherical volume through a small circular window is shorter if diffusion occurs along the periphery rather than through the internal volume. This result requires that the window be small compared to the size of the sphere, a condition that is approximately met by the mitotic yeast cell, especially if we assume that the mother-daughter tunnel is partially blocked by microtubules and chromosomes. Indeed, by computational simulation, we were able to recapitulate the increased plasmid segregation achieved by membrane tethering, if we restricted the random movement of the plasmid to a peripheral zone of the dividing nucleus. In this case, plasmid transmission to the daughter cell increased from 15% to 30%.

## Association with Telomeres Improves Plasmid Segregation

Previous models for facilitated segregation have invoked an alternative mechanism, namely, an association with chromosomes. This is thought to allow, for example, the Epstein-Barr virus to segregate mitotically [40]. Intriguingly, whereas the targeting of yku80 can anchor DNA to the NE in G1 and S phase cells [37], the targeting of lexA-ku80-9, a mutant form of yku80 that binds Sir4 [37], failed to relocate the internal lacO-tagged *ARS607* locus to the NE in G2 phase cells (Figure 4B). Nonetheless, its binding to pAA4 was able to enhance mitotic transmission of the plasmid to the daughter cell (Figure 4F). The effect required lexA binding sites on the plasmid (see pAA0, Figure 4D) and did not increase replication efficiency (Figure S4). Consistently, and unlike the targeting of lexA-Sir4PAD and lexA-Yif1, the stabilizing effect of yku80-9 required Sir4 (Figures 4E and 4F). The mitotic stability and plasmid loss rate results are summarized are summarized in Table 3.

We hypothesized that the targeting of yku80-9 to the plasmid bridges or tethers the episome to telomere-bound proteins, such as Sir4. To confirm this, we performed chromatin immunoprecipitation (ChIP) in a strain carrying a functional Myc-tagged copy of the telomere-specific protein Rif1. If lexA-yku80-9 links the pAA4 plasmid to telomeres, then plasmid DNA should be recovered with Rif1 after crosslinking

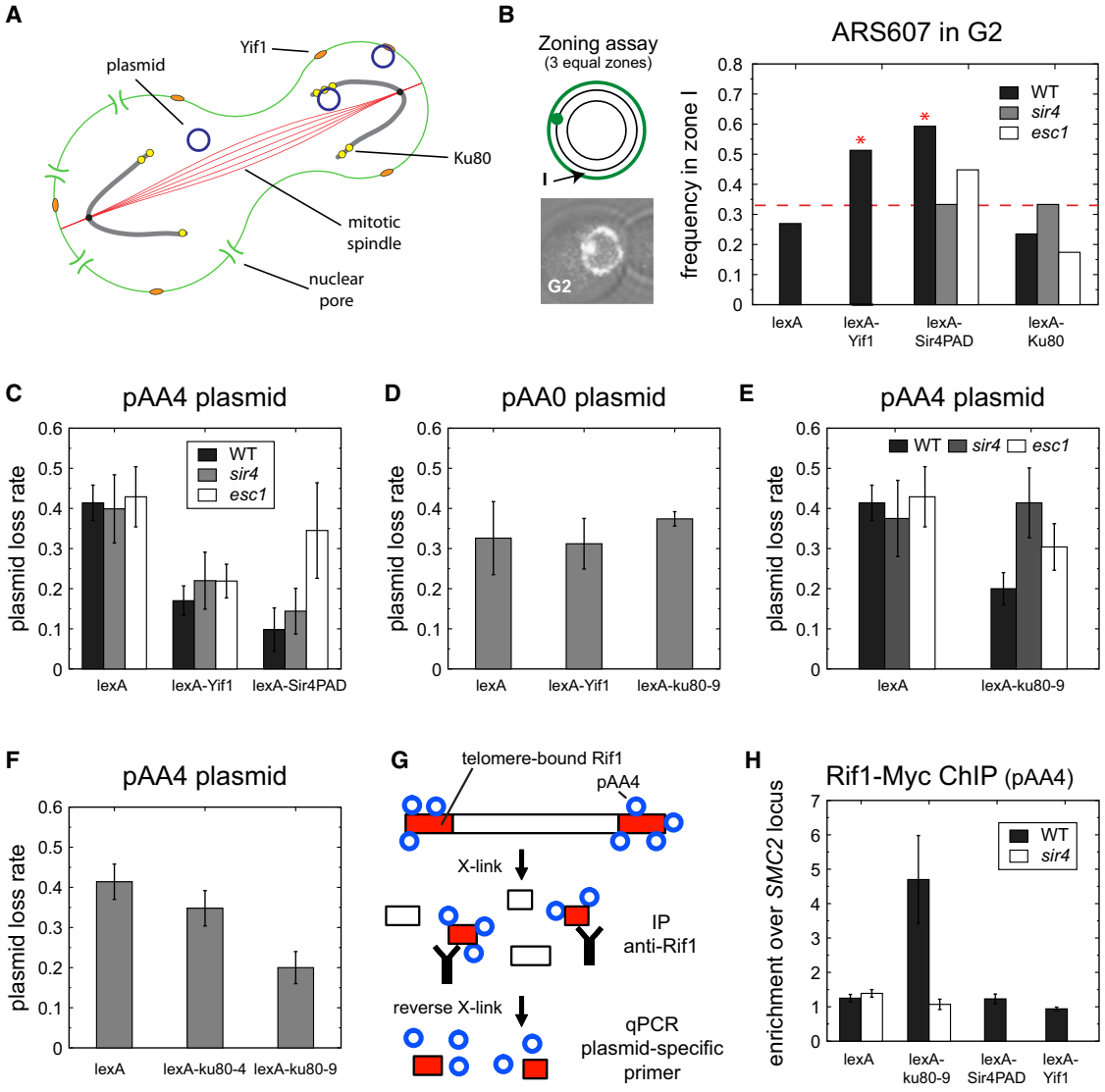


Figure 4. Attachment to Both the Nuclear Envelope and to Telomeres Improves Plasmid Partitioning

(A) Illustration of the dividing nucleus. Proteins can tether plasmids to the nuclear envelope or to telomeres to improve mitotic segregation. See Figure S3.

(B) The zoning assay is used to quantify the position of a tagged locus in an interphase nucleus by binning into one of three concentric zones of equal area [37]. The targeting of lexA-Yif1 (n = 39) and lexA-Sir4PAD (n = 27) to an internal locus (*ARS607*) leads to a significant enrichment (p = 0.01 and p = 0.002 versus targeting of lexA alone [n = 89]) at the nuclear periphery (zone 1). In contrast, lexA-yku80-9 (n = 85) relocates *ARS607* to the periphery in G1 and S phase [37], but not in G2. Identical assays were performed in strains deleted for *sir4* and *esc1*, with expected results [37].

(C) Effect of lexA-Yif1 targeting on the pAA4 plasmid loss rate. The average of six trials with independent transformants of strains GA-180 (wild-type), GA-2660 (*sir4*), and GA-2662 (*esc1*) is shown.

(D) Effect of lexA-Yif1 and lexA-yku80-9 binding on pAA0 (no LexA sites) under conditions as in (C). A control for altered copy number is shown in Figure S4.

(E) Effect of lexA-yku80-9 targeting on pAA4 stability in isogenic wild-type, *sir4* (GA-2660), and *esc1* (GA-2662) mutant strains under conditions as in (C).

(F) Effect of lexA-yku80-9 and lexA-yku80-4 targeting on the stability of pAA4. The plasmid loss rate represents the average of six trials with independent transformants.

(G) Scheme for chromatin immunoprecipitation (ChIP) assay to identify DNA associated with telomeres that are precipitated with Rif1-Myc in wild-type (GA-3633) and *sir4* (GA-3662) strains bearing pAA4 and a plasmid expressing lexA fusion proteins. Cells were arrested at mitosis with nocodazole prior to formaldehyde fixation.

(H) Rif1-Myc ChIP was enriched 4.5-fold for the pAA4 signal over a genomic control locus (*SMC2*) only when lexA-ku80-9 bound the plasmid. Each value was normalized to the input fraction (total prior to IP). The mean of four independent transformants from two separate experiments is shown.

Error bars indicate standard error of the mean.

(Figure 4G). Using strains that carry pAA4 along with lexA-Yif1, lexA-Sir4PAD, or lexA-yku80-9, we found that only the yku80-9-bound plasmid was efficiently recovered in a ChIP for telomere-bound Rif1 (~4.5-fold enrichment; Figure 4H). Telomere association, like the decrease in plasmid loss rate, was abolished by *SIR4* deletion (Figures 4E and 4H). Consistently, another mutant form of yku80, lexA-yku80-4, which does not bind Sir4 [37], failed to improve plasmid segregation. We conclude that anchoring to telomeres is another means of enhancing episome transmission, overcoming the asymmetry inherent to the geometry and kinetics of budding yeast mitosis.

Table 2. Targeting of the Plasmid to the Nuclear Envelope by Yif1 Improves Segregation

| Plasmid | Genotype | lexA Fusion | Mitotic Stability (%) | Plasmid Loss Rate |
|---|---|---|---|---|
| pAA4 | wild-type | lexA | 10.4 ± 3.4 | 0.41 ± 0.04 |
| | | lexA-Yif1 | 33.2 ± 5.2 | 0.17 ± 0.04 |
| pAA4 | *sir4* | lexA | 7.4 ± 1.4 | 0.38 ± 0.1 |
| | | lexA-Yif1 | 28.6 ± 2.3 | 0.19 ± 0.06 |
| pAA4 | *esc1* | lexA | 6.8 ± 2.7 | 0.43 ± 0.08 |
| | | lexA-Yif1 | 19.3 ± 2.8 | 0.22 ± 0.04 |
| pAA0 | wild-type | lexA | 15.1 ± 3.2 | 0.33 ± 0.09 |
| | | lexA-Yif1 | 17.0 ± 5.8 | 0.31 ± 0.06 |

Data are presented as mean ± standard deviation.

Table 3. lexA-yku80-9 Targeting Improves Plasmid Segregation

| Plasmid | Genotype | lexA Fusion | Mitotic Stability (%) | Plasmid Loss Rate |
|---|---|---|---|---|
| pAA4 | wild-type | lexA | 10.4 ± 3.4 | 0.41 ± 0.04 |
| | | lexA-yku80-9 | 42.1 ± 8.1 | 0.2 ± 0.04 |
| pAA4 | *sir4* | lexA | 7.4 ± 1.4 | 0.38 ± 0.1 |
| | | lexA-yku80-9 | 7.1 ± 2.2 | 0.41 ± 0.09 |
| pAA4 | *sir3* | lexA | 7.7 ± 1.6 | 0.39 ± 0.07 |
| | | lexA-yku80-9 | 12.2 ± 3.3 | 0.35 ± 0.08 |
| pAA4 | *esc1* | lexA | 6.8 ± 2.7 | 0.43 ± 0.08 |
| | | lexA-yku80-9 | 23.4 ± 6.5 | 0.30 ± 0.06 |
| pAA0 | wild-type | lexA | 15.1 ± 3.2 | 0.33 ± 0.09 |
| | | lexA-yku80-9 | 20.4 ± 3.3 | 0.37 ± 0.02 |

Data are presented as mean ± standard deviation.

## Discussion

In this study, we have shown that in yeast, both extrachromosomal rings and ARS plasmids move freely inside the nucleus. Nonetheless, they show a strong segregation bias, segregating 10 times more efficiently to the mother cell. Computational simulations based on empirical parameters of nuclear size and shape, diffusion rates, and the length of mitosis led us to propose that the shape of the dividing nucleus might impose a substantial constraint on an episome's mother-daughter transition by passive diffusion. This constraint would be aggravated by the brevity of budding yeast mitosis (10 min at 30°C). Indeed, simulations show that the episome would not reach an equilibrium between mother and daughter in this period. We confirmed our predictions by showing that the stability of an ARS plasmid is increased by extending the duration of mitosis, with two unrelated mutations and by a reduction in growth temperature.

The computational modeling of the plasmid transition from mother to daughter was based on unobstructed diffusion in the dividing nucleus. From our results, we predict that a "diffusional barrier" could arise from the geometry of the dividing nucleus. Although we do not exclude that other parameters contribute to the mother-daughter segregation bias detected for a freely diffusing ARS plasmid, our data show that this bias can be largely accounted for by structural features of the bud neck, which inhibit the efficient diffusion of episomes into the daughter nucleus.

We confirmed an earlier observation that the deletion of *BUD6*, which leads to a thicker bud neck [31], increases plasmid stability [22]. However, we found that the deletion of *BUD6* also extends G2/M phase considerably. Thus, although the absence of Bud6 does affect bud-neck morphology [31], its effect on G2/M transition is even more pronounced. We tried to suppress the *bud6* accumulation in mitosis by deletion of *swe1* [41], yet this did not alter the cell-cycle distribution of cells as detected by fluorescence-activated cell sorting, nor did it alter the improvement of *LYS2* ring segregation provoked by deletion of *bud6* (Figure S5). Thus, the stabilizing effect of *bud6* deletion on plasmid transmission, like that of the *yku70* mutation, is most likely accounted for by the prolonged mitosis, with or without bud-neck variation.

Earlier work argued that centromere-excised plasmids would associate with nuclear pores, which segregate asymmetrically into the mother as a result of a Bud6-dependent diffusion barrier at the bud neck [22]. However, Khmelinskii et al. [23] recently showed that mother cells do not retain nuclear pores, and in an accompanying paper in this issue of *Current Biology*, this group further shows that the artificial anchorage of plasmid to nuclear pore actually improves mitotic segregation [38]. This is fully consistent with our data (Figure 4). We show here that freely moving excised chromatin rings and ARS plasmids retain a strongly asymmetric mitotic distribution into the mother cell without pore association.

It is unclear why Shcheprova et al. [22] failed to observe free plasmid diffusion in their system, but it likely stems from the use of a CEN-ARS plasmid from which the centromeric sequence is excised. Because centromeres in budding yeast have been shown to interact with the NE-embedded spindle pole body [42], it is possible that their plasmid—even after excision of the centromere—remains bound to the spindle pole body, as a result of centromere-induced chromatin marks. In contrast, our system exploits episomes that have never contained centromeres.

We argue that the retention of ARS plasmids in the mother nucleus does not require an active mechanism and occurs passively as a result of the geometric constraints that the mitotic nucleus imposes on plasmid diffusion. We find that diffusion coefficients of plasmids should have an effect on segregation, as shown by an earlier study in which the small 1.45 kb *TRP1* circle was shown to lose its segregation bias [24].

How do noncentromeric episomes overcome the segregation bias? By targeting the telomere anchoring factor Sir4PAD, Gartenberg and colleagues suggested that interaction with Esc1 would improve segregation [26, 36]. Esc1 is not a transmembrane protein but is efficiently associated with the NE [37]. We show here that association with either the NE or telomeres in G2/M increases the mitotic transmission of an episome. Thus, the segregation of the nuclear envelope, like the segregation of chromosomes, can be a mechanism of DNA partitioning. This may well contribute to mechanisms of aging and daughter cell rejuvenation.

It has been proposed that cell polarity might have arisen originally as a solution to cope with the accumulation of damaged proteins and DNA, which are caused by vital cellular activities [1, 4]. Indeed, the asymmetric division of the budding yeast nucleus together with the limited duration of mitosis provides the cell with a powerful mechanism to retain detrimental material in the mother nucleus. Although there are many other mechanisms contributing to aging in yeast, the geometry and kinetics of budding yeast mitosis appear to ensure asymmetric distribution of nuclear contents. This may help rejuvenate daughter cells and generate an immortal population. Episomes, which are not essential to the propagation of the species, accumulate in mother cells unless they possess a means of passing piggyback with segregating components of the cell. A default system for passive retention

of cellular components resulting from geometrical and kinetic constraints may well be relevant to other systems of asymmetric segregation found in development throughout the animal kingdom.

### Supplemental Information

Supplemental Information includes one table, five figures, and Supplemental Experimental Procedures and can be found with this article online at doi:10.1016/j.cub.2010.12.016.

### Acknowledgments

We would like to thank Marc Gartenberg for extensive assistance and advice, Elisa Varela for assistance with immunostaining, and the Gasser laboratory for constructive criticism. Support from the Novartis Research Foundation, the National Center for Competence in Research "Frontiers in Genetics" and European Union Network of Excellence "Epigenome," and a European Molecular Biology Organization long-term fellowship to A.T. is gratefully acknowledged.

Received: September 6, 2010
Revised: November 10, 2010
Accepted: December 8, 2010
Published online: December 30, 2010

### References

1. Partridge, L., and Barton, N.H. (1993). Optimality, mutation and the evolution of ageing. Nature *362*, 305–311.
2. Gönczy, P., and Rose, L.S. (2005). Asymmetric cell division and axis formation in the embryo. In WormBook, The *C. elegans* Research Community, ed. 10.1895/wormbook.1.30.1, http://www.wormbook.org.
3. Sinclair, D.A., and Guarente, L. (1997). Extrachromosomal rDNA circles—a cause of aging in yeast. Cell *91*, 1033–1042.
4. Ackermann, M., Stearns, S.C., and Jenal, U. (2003). Senescence in a bacterium with asymmetric division. Science *300*, 1920.
5. Hernebring, M., Brolén, G., Aguilaniu, H., Semb, H., and Nyström, T. (2006). Elimination of damaged proteins during differentiation of embryonic stem cells. Proc. Natl. Acad. Sci. USA *103*, 7700–7705.
6. Müller, I. (1985). Parental age and the life-span of zygotes of Saccharomyces cerevisiae. Antonie van Leeuwenhoek *51*, 1–10.
7. Kennedy, B.K., Gotta, M., Sinclair, D.A., Mills, K., McNabb, D.S., Murthy, M., Pak, S.M., Laroche, T., Gasser, S.M., and Guarente, L. (1997). Redistribution of silencing proteins from telomeres to the nucleolus is associated with extension of life span in S. cerevisiae. Cell *89*, 381–391.
8. McMurray, M.A., and Gottschling, D.E. (2003). An age-induced switch to a hyper-recombinational state. Science *301*, 1908–1911.
9. Jazwinski, S.M. (1993). The genetics of aging in the yeast Saccharomyces cerevisiae. Genetica *91*, 35–51.
10. Kennedy, B.K., Austriaco, N.R., Jr., and Guarente, L. (1994). Daughter cells of Saccharomyces cerevisiae from old mothers display a reduced life span. J. Cell Biol. *127*, 1985–1993.
11. Aguilaniu, H., Gustafsson, L., Rigoulet, M., and Nyström, T. (2003). Asymmetric inheritance of oxidatively damaged proteins during cytokinesis. Science *299*, 1751–1753.
12. Laun, P., Pichova, A., Madeo, F., Fuchs, J., Ellinger, A., Kohlwein, S., Dawes, I., Fröhlich, K.U., and Breitenbach, M. (2001). Aged mother cells of Saccharomyces cerevisiae show markers of oxidative stress and apoptosis. Mol. Microbiol. *39*, 1166–1173.
13. Lai, C.Y., Jaruga, E., Borghouts, C., and Jazwinski, S.M. (2002). A mutation in the ATP2 gene abrogates the age asymmetry between mother and daughter cells of the yeast Saccharomyces cerevisiae. Genetics *162*, 73–87.
14. Falcón, A.A., and Aris, J.P. (2003). Plasmid accumulation reduces life span in Saccharomyces cerevisiae. J. Biol. Chem. *278*, 41607–41617.
15. Sinclair, D.A., Mills, K., and Guarente, L. (1997). Accelerated aging and nucleolar fragmentation in yeast *sgs1* mutants. Science *277*, 1313–1316.
16. Defossez, P.A., Prusty, R., Kaeberlein, M., Lin, S.J., Ferrigno, P., Silver, P.A., Keil, R.L., and Guarente, L. (1999). Elimination of replication block protein Fob1 extends the life span of yeast mother cells. Mol. Cell *3*, 447–455.
17. Kaeberlein, M., McVey, M., and Guarente, L. (1999). The SIR2/3/4 complex and SIR2 alone promote longevity in Saccharomyces cerevisiae by two different mechanisms. Genes Dev. *13*, 2570–2580.
18. Kim, S., Benguria, A., Lai, C.Y., and Jazwinski, S.M. (1999). Modulation of life-span by histone deacetylase genes in Saccharomyces cerevisiae. Mol. Biol. Cell *10*, 3125–3136.
19. Murray, A.W., and Szostak, J.W. (1983). Pedigree analysis of plasmid segregation in yeast. Cell *34*, 961–970.
20. Gordon, C.N. (1977). Chromatin behaviour during the mitotic cell cycle of Saccharomyces cerevisiae. J. Cell Sci. *24*, 81–93.
21. Heun, P., Laroche, T., Shimada, K., Furrer, P., and Gasser, S.M. (2001). Chromosome dynamics in the yeast interphase nucleus. Science *294*, 2181–2186.
22. Shcheprova, Z., Baldi, S., Frei, S.B., Gonnet, G., and Barral, Y. (2008). A mechanism for asymmetric segregation of age during yeast budding. Nature *454*, 728–734.
23. Khmelinskii, A., Keller, P.J., Lorenz, H., Schiebel, E., and Knop, M. (2010). Segregation of yeast nuclear pores. Nature *466*, E1.
24. Zakian, V.A., and Kupfer, D.M. (1982). Replication and segregation of an unstable plasmid in yeast. Plasmid *8*, 15–28.
25. Gartenberg, M.R., Neumann, F.R., Laroche, T., Blaszczyk, M., and Gasser, S.M. (2004). Sir-mediated repression can occur independently of chromosomal and subnuclear contexts. Cell *119*, 955–967.
26. Ansari, A., and Gartenberg, M.R. (1997). The yeast silent information regulator Sir4p anchors and partitions plasmids. Mol. Cell. Biol. *17*, 7061–7068.
27. Lord, P.G., and Wheals, A.E. (1981). Variability in individual cell cycles of Saccharomyces cerevisiae. J. Cell Sci. *50*, 361–376.
28. Longtine, M.S., Enomoto, S., Finstad, S.L., and Berman, J. (1992). Yeast telomere repeat sequence (TRS) improves circular plasmid segregation, and TRS plasmid segregation involves the RAP1 gene product. Mol. Cell. Biol. *12*, 1997–2009.
29. Heideker, J., Lis, E.T., and Romesberg, F.E. (2007). Phosphatases, DNA damage checkpoints and checkpoint deactivation. Cell Cycle *6*, 3058–3064.
30. Maringele, L., and Lydall, D. (2002). EXO1-dependent single-stranded DNA at telomeres activates subsets of DNA damage and spindle checkpoint pathways in budding yeast yku70Delta mutants. Genes Dev. *16*, 1919–1933.
31. Amberg, D.C., Zahner, J.E., Mulholland, J.W., Pringle, J.R., and Botstein, D. (1997). Aip3p/Bud6p, a yeast actin-interacting protein that is involved in morphogenesis and the selection of bipolar budding sites. Mol. Biol. Cell *8*, 729–753.
32. Vanoni, M., Vai, M., and Frascotti, G. (1984). Effects of temperature on the yeast cell cycle analyzed by flow cytometry. Cytometry *5*, 530–533.
33. Coffey, W.T., Kalmykov, Y.P., and Waldron, J.T. (2004). The Langevin Equation, Second Edition (Singapore: World Scientific Publishing).
34. Aleksandrov, A.A., and Trakhtengerts, M.S. (1974). Viscosity of water at temperatures of −20 to 150°C. J. Eng. Phys. Thermophys. *27*, 1235–1239.
35. Longtine, M.S., Enomoto, S., Finstad, S.L., and Berman, J. (1993). Telomere-mediated plasmid segregation in Saccharomyces cerevisiae involves gene products required for transcriptional repression at silencers and telomeres. Genetics *133*, 171–182.
36. Andrulis, E.D., Zappulla, D.C., Ansari, A., Perrod, S., Laiosa, C.V., Gartenberg, M.R., and Sternglanz, R. (2002). Esc1, a nuclear periphery protein required for Sir4-based plasmid anchoring and partitioning. Mol. Cell. Biol. *22*, 8292–8301.
37. Taddei, A., Hediger, F., Neumann, F.R., Bauer, C., and Gasser, S.M. (2004). Separation of silencing from perinuclear anchoring functions in yeast Ku80, Sir4 and Esc1 proteins. EMBO J. *23*, 1301–1312.
38. Khmelinskii, A., Meurer, M., Knop, M., and Schiebel, E. (2011). Artificial tethering to nuclear pores promotes partitioning of extrachromosomal DNA during yeast asymmetric cell division. Curr. Biol. *21*, this issue, R17–R18.
39. Singer, A., Schuss, Z., Holcman, D., and Eisenberg, R. (2006). Narrow Escape, Part I. J. Stat. Phys. *122*, 437–463.
40. Kapoor, P., Lavoie, B.D., and Frappier, L. (2005). EBP2 plays a key role in Epstein-Barr virus mitotic segregation and is regulated by aurora family kinases. Mol. Cell. Biol. *25*, 4934–4945.
41. Sheu, Y.J., Barral, Y., and Snyder, M. (2000). Polarized growth controls cell shape and bipolar bud site selection in Saccharomyces cerevisiae. Mol. Cell. Biol. *20*, 5235–5247.
42. Jaspersen, S.L., and Winey, M. (2004). The budding yeast spindle pole body: Structure, duplication, and function. Annu. Rev. Cell Dev. Biol. *20*, 1–28.